

Bond-orbital theory of linear and nonlinear electronic response in ionic crystals.

I. Linear response

M. E. Lines

AT&T Bell Laboratories, Murray Hill, New Jersey 07974-2070

(Received 26 May 1989; revised manuscript received 14 September 1989)

Materials characterization for optical device purposes relies heavily on a knowledge of material compliances related to dielectric response. These include both linear response (dielectric constant) and various orders of nonlinear response involving electro-optics (Kerr and Pockels effects, harmonic generation, etc.) and elasto-optics (light scattering, piezoelectrics, etc.) All these properties follow, in principle, from an adequate description of electronic bonding in insulators and semiconductors. This paper sets out a bond-orbital theory of dielectric response which, it is anticipated, will eventually lead to a global semiquantitative representation of all these various properties as functions of such readily available measures as formal valency, bond length, ionic radii, etc. In its initial form, as presented here, it is used to obtain just such an expression for the electronic dielectric constant of pretransition-metal halides and chalcogenides. The root-mean-square accuracy, over 28 halides, is 2.4% and over 44 materials in all, about 3.4%. In the companion paper (II) a similar calculation is carried out for nonlinear response on the same materials.

I. INTRODUCTION

It is with some concern when I note that even the most recently revised introductory graduate texts on solid-state physics¹ still discuss electronic response in insulators in terms of the supposedly environmentally independent electronic polarizabilities α_i of their ionic constituents and include a table associating polarizability values with ion types. The association is made via the Clausius-Mossotti (or Lorentz-Lorenz) relationship

$$(\epsilon - 1)/(\epsilon + 2) = (4\pi/3) \sum_i N_i \alpha_i, \quad (1.1)$$

where ϵ is the electronic dielectric constant (equal to the square of the refractive index) and N_i is the number of ions of type i per unit volume. However, it is now clear from the literature²⁻⁶ that any formulation based on a summation \sum_i over independent ionic contributions α_i must recognize an essential environmental dependence of α_i which precludes any viable one-to-one association of α_i with ion types.

Although the details of the formula include the assumption of a local-field enhancement of Lorentz form,¹ the assumed environmental independence of α_i rests on an even more basic premise; namely that the dominant electronic excitations (real or virtual) which are produced by an optical frequency electric field are wholly *intraionic*. Only in this circumstance could the notion of uniquely defined (i.e., approximately composition-independent) ionic polarizabilities α_i be developed. However, as first noted by Pantelides,⁷ a careful analysis of experimental data for optical response over a wide range of insulators clearly excludes the independent-ion model. Moreover, this finding is hardly surprising when the lowest-energy electronic excitations (whether to exciton or lower

conduction-band levels) are known to be dominated by charge-transfer processes.^{8,9}

But Pantelides⁷ went further to suggest that the experimental evidence actually points to the opposite extreme condition; a marked dominance of *interion* over *intraion* processes in the optical response of insulators. If true, this would suggest that a theory based solely upon *interion* excitations should be more fundamental than any additive polarizable-ion model. It is the purpose of the present (I) and following (II) papers to develop the simplest possible theory of this nature for both linear and nonlinear response, to test its accuracy and limitations, and to derive relationships of textbook simplicity to replace their "independent-ion" counterparts, at least over wide classes of insulator.

Although, with the use of ultrafast computing facilities, it is now becoming possible to calculate electronic structure and associated dielectric response from first principles for all classes of simple solids (from molecular to metallic¹⁰⁻¹⁵), such *ab initio* methods involve highly sophisticated machine computation and are therefore somewhat arcane and certainly not physically transparent at the introductory graduate level. In addition, their numerical findings are not well adapted for the organization of chemical trends. As a result, the various semiempirical models that have been developed over the years^{9,16-22} (which attempt to retain the essentials of the underlying physics for each material class while simplifying the analysis to bare essentials) still have important roles to play.

For binary semiconductors and insulators the two competing (but possibly not conflicting¹⁶) models are those of Phillips^{17,18} and of Harrison and co-workers.^{9,20-22} The first is based upon a single band gap in free-electron bands while the second adopts a local picture of bonding and antibonding orbitals formed by in-

interactions between nearest-neighbor anion and cation wave functions. In this paper we wish to develop the bond-orbital method since, not only is it extremely transparent in the physical approximations which it pursues, but also (surprisingly) it has never been presented for insulators due to a persistent belief that *independent* bond orbitals (which are not present in highly coordinated insulator complexes) are a necessary ingredient of the method; they are not.

The bond-orbital method was developed initially for binary covalent (tetrahedrally bonded) semiconductors and later extended to other covalent structures.^{23,24} The work of the present paper, while inspired by Harrison's earlier formalism, differs from it in a number of ways. First, it includes orbital overlap in an essential fashion (i.e., in a manner which cannot simply be absorbed into a rescaling of other parameters). Secondly, it recognizes the differences in size of the cation and anion orbitals which combine to form the bond orbitals. This size difference is absolutely essential for discussing electronic response in insulators, for which ionic radii can differ by more than a factor of 2. Thirdly, and most importantly, it empirically relates one-electron matrix elements to physical and chemical trends in a manner which completely rids the final equations of any further *ad hoc* parametrization. Finally, in conjunction with the paper to follow, it settles the question of local-field enhancement (Lorentzian or otherwise) in favor of its essential absence in the context of bond-orbital theory.

II. FORMAL BOND-ORBITAL THEORY IN THE ABSENCE OF APPLIED FIELD

Consider a binary insulator or semiconductor MX_n , where M denotes the metal (or cation) species and X the anion species. Limiting ourselves, for the present, to structures which possess only a single class of equivalent primary $M-X$ bonds, we express such a representative bond as a linear combination of a single pair of unspecified atomic orbitals $|h_M\rangle$ and $|h_X\rangle$ associated, respectively, with the metal and the anion. Although it is anticipated, for the class of materials of immediate concern in this paper, that $|h_X\rangle$ is predominantly of p -orbital character and $|h_M\rangle$ largely (though possibly less dominantly) of s -orbital form, it is not necessary to impose these restrictions in the formalism which will be cast solely in terms of parameters representing matrix elements within and between these atomic orbitals.

Following, initially, the formulation developed by Harrison and co-workers^{20,21} for covalent semiconductors (in which $|h_M\rangle$ and $|h_X\rangle$ were sp^3 hybrids), we first consider a σ bond between the metal and an arbitrary nearest-neighbor anion, and write a normalized bonding orbital $|b_0\rangle$ as the linear combination

$$|b_0\rangle = u_M |h_M\rangle + u_X |h_X\rangle . \quad (2.1)$$

The coefficients u_M and u_X are then obtained as functions of the relevant interorbital and intraorbital matrix elements, by variationally minimizing the bond-orbital energy $\langle b_0 | \mathcal{H}_0 | b_0 \rangle / \langle b_0 | b_0 \rangle$ with respect to them, where H_0 is the one-electron Hamiltonian. This Hamiltonian may,

in a first approximation, be assumed to consist of a kinetic-energy operator and interactions with the M -cation and X -anion nuclei and electrons.

Defining the one-electron matrix elements

$$\langle h_M | \mathcal{H}_0 | h_M \rangle = - \langle h_X | \mathcal{H}_0 | h_X \rangle = E_0 , \quad (2.2)$$

$$\langle h_M | \mathcal{H}_0 | h_X \rangle = -M , \quad (2.3)$$

where the former also selects an arbitrary zero of absolute-energy scale, and the overlap integrals

$$\langle h_M | h_M \rangle = \langle h_X | h_X \rangle = 1 , \quad (2.4)$$

$$\langle h_M | h_X \rangle = S , \quad (2.5)$$

we now differentiate the energy function

$$E = \frac{\langle b_0 | \mathcal{H}_0 | b_0 \rangle}{\langle b_0 | b_0 \rangle} , \quad (2.6)$$

partially with respect to u_M and u_X of Eq. (2.1) to obtain the stationary conditions

$$\begin{pmatrix} E + E_0 & M + ES \\ M + ES & E - E_0 \end{pmatrix} \begin{pmatrix} u_X \\ u_M \end{pmatrix} = \begin{pmatrix} 0 \\ 0 \end{pmatrix} . \quad (2.7)$$

The matrix equation (2.7) has nontrivial solutions when the determination of the coefficients is set equal to zero, viz.,

$$\begin{vmatrix} E + E_0 & M + ES \\ M + ES & E - E_0 \end{vmatrix} = 0 . \quad (2.8)$$

Of the two solutions for E , which follow in the form

$$E_{\pm} = SV_2 \pm (V_2^2 + V_3^2)^{1/2} , \quad (2.9)$$

where

$$V_2 = M / (1 - S^2) , \quad (2.10)$$

and

$$V_3 = E_0 / (1 - S^2)^{1/2} , \quad (2.11)$$

the smaller, $E = E_- = E_{\text{bond}}$, defines the energy of the bonding orbital. Substitution of $E = E_{\text{bond}}$ into Eq. (2.8) now supplies the corresponding bond-orbital coefficients in the form

$$u_M = \pm [(q_0 - r_0) / 2]^{1/2} , \quad (2.12)$$

$$u_X = [(q_0 + r_0) / 2]^{1/2} , \quad (2.13)$$

in which

$$q_0 = (1 - S\alpha) / (1 - S^2) , \quad (2.14)$$

$$r_0 = [(1 - \alpha^2) / (1 - S^2)]^{1/2} , \quad (2.15)$$

where

$$\alpha = V_2 / (V_2^2 + V_3^2)^{1/2} . \quad (2.16)$$

The + (−) sign for u_M in Eq. (2.12) holds for $\alpha > S$ ($\alpha < S$) and the bonding wave function $|b_0\rangle$ has been normalized to unity according to

$$\langle b_0 | b_0 \rangle = u_X^2 + u_M^2 + 2u_X u_M S = 1. \quad (2.17)$$

The parameter α of Eq. (2.16) can be used as a measure of covalency by noting that full covalency ($u_M = u_X$, $r_0 = 0$) corresponds to $\alpha = 1$, $V_3/V_2 = 0$, while the opposite formal limit $V_2/V_3 = 0$ of complete ionicity leads to $\alpha = 0$. However, the two limits differ in relevance since, while $V_3/V_2 = 0$ is physically realized in the elemental semiconductors, the opposite limit $V_2/V_3 = 0$ is never approached by any known chemical bond. In fact, the most ionic materials (namely the alkali halides) are known to have bonding orbitals (or equivalently valence bands) which are overwhelmingly of anionic p character.²⁵ This points to the conditions $u_X = 1$, $u_M = 0$, $q_0 = r_0$, (or equivalently $\alpha = S$) as being close to the practical ionic limit for real systems. Accordingly we shall, from this point on, refer to the condition

$$|b_0\rangle = |h_X\rangle, \quad \alpha = S, \quad (2.18)$$

as being the "ionic limit" for solids. Note that in this limit the corresponding antibonding orbital is the orthogonal $|a_0\rangle = |h_M\rangle - S|h_X\rangle$.

It follows that, as a measure of covalency, α can take on values only between S and unity, where the overlap S , as we shall see, may vary somewhat from material to material, but is typically of order 0.3–0.45 for insulators. It also follows that for all physical bonds it is the positive sign in Eq. (2.12) which is relevant.

III. THE BONDING ORBITAL MOMENT

In order to calculate the dielectric response to an applied field, it is first necessary to consider the magnitude of the dipole moment of the bonding orbital $|b_0\rangle$ of Eq. (2.1). Measuring distance x along a bond from the cation nucleus $x = 0$ to the anion nucleus $x = d$, we can express this electric dipole moment (per one electron orbital) as

$$\begin{aligned} \langle b_0 | ex | b_0 \rangle = & u_M^2 \langle h_M | ex | h_M \rangle + u_X^2 \langle h_X | ex | h_X \rangle \\ & + 2u_M u_X \langle h_M | ex | h_X \rangle, \end{aligned} \quad (3.1)$$

where e is the electronic charge. The formalism simplifies if x is recast in terms of distance from the point $x = x_0$ along the bond at which the matrix element $\langle h_M | (x - x_0) | h_X \rangle$ vanishes; viz.,

$$x_0 = \frac{\langle h_M | x | h_X \rangle}{\langle h_M | h_X \rangle}. \quad (3.2)$$

In the new formalism, and using Eqs. (2.12) and (2.13), the dipole moment of Eq. (3.1) now can be written

$$\begin{aligned} \langle b_0 | e(x - x_0) | b_0 \rangle = & [(q_0 - r_0)/2] \langle h_M | e(x - x_0) | h_M \rangle \\ & + [(q_0 + r_0)/2] \langle h_X | e(x - x_0) | h_X \rangle. \end{aligned} \quad (3.3)$$

Assuming $|h_M\rangle$ and $|h_X\rangle$ for the alkali halides and alkaline-earth chalcogenides to be centered at the cation ($x = 0$) and anion ($x = d$) nuclei respectively, Eq. (3.3) further reduces to

$$\langle b_0 | e(x - x_0) | b_0 \rangle = (e/2)(r_0 d + q_0 \Delta), \quad (3.4)$$

where

$$\Delta = d - 2x_0 \quad (3.5)$$

or, equivalently

$$(d + \Delta)/d = 2[1 - (x_0/d)]. \quad (3.6)$$

Now, while d (the bond length) is clearly a measurable quantity, the nature of the distance variable x_0 is not so self-evident in a general context. In the limit of full covalency, in homopolar semiconductors such as Si or Ge, it is obvious by symmetry [see Fig. 1(a)] that $x_0 = d/2$ and hence $\Delta = 0$. This is the value used by Harrison and co-workers^{20–22} for all the tetrahedrally bonded (sp^3 -hybrid) semiconductors. Whether or not this is an appropriate assumption for the wider field of sp^3 semiconductors is a topic which we shall take up in a future publication. Regardless of this question we shall demonstrate below that, for the more ionic materials of concern in this and the following paper, the condition $x_0 = d/2$ is clearly inappropriate.

In essence, x_0 locates approximately the center of the region of maximum overlap of the cationic and anionic wave functions $|h_M\rangle$ and $|h_X\rangle$, see Fig. 1(b). As the size of the anionic orbital increases for a fixed cation, the peak overlap position (and hence x_0) will clearly move to smaller values, and $(d + \Delta)/d$ of Eq. (3.6) to larger values. In a complementary fashion, as the size of the cationic orbital increases for fixed anion, peak overlap will move to larger values, and $(d + \Delta)/d$ to smaller ones.

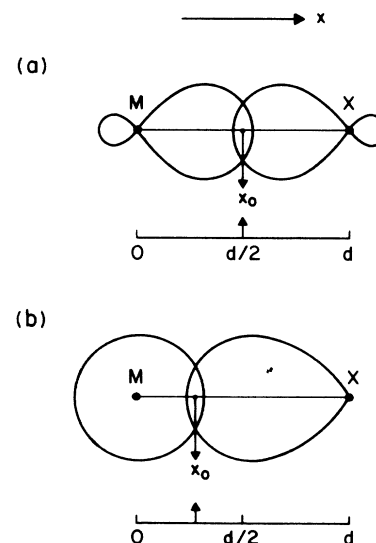


FIG. 1. (a) Schematic representing the overlap of two identical sp^3 hybrids, with respective origins at M ($x = 0$) and X ($x = d$), showing the location ($x = x_0 = d/2$) of their region of maximum overlap. (b) An analogous schematic for a cation s orbital, centered at M , and an anion p_x orbital, centered at X (only the left-hand lobe shown), with maximum overlap at $x = x_0 < d/2$.

The quantitative manner in which this occurs will be established empirically (Sec. V) as follows:

$$(d + \Delta)/d = [(R_X + R_M)/2R_M]^{1/2} = (d/2R_M)^{1/2}, \quad (3.7)$$

where R_X and R_M are, respectively, the ionic radii of the anion and cation with $R_M + R_X = d$. It follows that

$$\Delta/d = (d/2R_M)^{1/2} - 1, \quad (3.8)$$

and

$$x_0/d = 1 - (d/8R_M)^{1/2}. \quad (3.9)$$

Clearly, when $R_X = R_M = d/2$, then $x_0 = d/2$ and $\Delta = 0$.

IV. LINEAR DIELECTRIC RESPONSE

We now examine the response of a representative σ -bonding orbital $|b\rangle$ to an applied electric field fE_x along the bond direction x , where the factor f absorbs any local-field enhancement or shielding effects. In the presence of the field, a term $-efE_x(x - x_0)$ must be added to the original zero-field one-electron Hamiltonian \mathcal{H}_0 of Sec. II. Led by the form [Eqs. (2.1), (2.12), and (2.13)] adopted by the zero-field bonding orbital $|b_0\rangle$, we express the new field-dependent bond orbital $|b\rangle$ in the analogous manner

$$|b\rangle = [(q-r)/2]^{1/2}|h_M\rangle + [(q+r)/2]^{1/2}|h_X\rangle, \quad (4.1)$$

but where now q and r are field-dependent quantities to be determined, and which reduce necessarily to q_0 and r_0 , respectively, when E_x goes to zero.

Using the form Eq. (4.1), the field-dependent bonding energy

$$E = \langle b | [\mathcal{H}_0 - efE_x(x - x_0)] | b \rangle \quad (4.2)$$

can now be expanded directly in terms of the zero-field matrix elements of Sec. II and the bond length parameters d and Δ of Sec. II in the form

$$E = -rV_3a - (q^2 - r^2)^{1/2}V_2a^2 - (\lambda/2)(rd + q\Delta), \quad (4.3)$$

in which

$$a = (1 - S^2)^{1/2}, \quad (4.4)$$

and

$$\lambda = efE_x. \quad (4.5)$$

Relating r and q via their bond-orbital normalization condition $\langle b | b \rangle = 1$, viz.,

$$qa^2 = 1 - S(1 - r^2a^2)^{1/2}, \quad (4.6)$$

we can now eliminate q from Eq. (4.3) to obtain

$$E = -rV_3a - V_2[-S + (1 - r^2a^2)^{1/2}] - (\lambda/2)rd - (\lambda/2)(\Delta/a^2)[1 - S(1 - r^2a^2)^{1/2}]. \quad (4.7)$$

Expanding r as a Taylor series in field parameter λ , i.e.,

$$r = r_0 + \sum_{n=1}^{\infty} r_n \lambda^n, \quad (4.8)$$

now enables us to evaluate r_n (for any order n) by minimizing successive coefficients of λ^n (i.e., $n = 0, 1, 2, 3, \dots$) in the expansion of the energy E of Eq. (4.7) with respect to r_n ; that is, via a general energy-minimization procedure. The algebraic manipulations are tedious though straightforward and we find, to third order in n

$$r_0 = (1 - \alpha^2)^{1/2}/a, \quad (4.9)$$

$$r_1 = \alpha^3 A / 2V_2 a^2, \quad (4.10)$$

$$r_2 = -\alpha^3 AB / 8V_2^2 a^3, \quad (4.11)$$

$$r_3 = \alpha^4 AC / 16V_2^3 a^4, \quad (4.12)$$

where

$$A = d + (\Delta S / a\alpha)(1 - \alpha^2)^{1/2}, \quad (4.13)$$

$$B = 3\alpha(1 - \alpha^2)^{1/2}d + (\Delta S / a)(1 - 3\alpha^2), \quad (4.14)$$

$$C = \alpha d^2(4 - 5\alpha^2) + 2(d\Delta S / a)(1 - 5\alpha^2)(1 - \alpha^2)^{1/2} + \alpha(\Delta S / a)^2(5\alpha^2 - 3). \quad (4.15)$$

The zeroth-order solution r_0 is simply a regeneration of the Sec. II finding of Eq. (2.15). Defining linear ($n = 1$) and nonlinear ($n > 1$) bond-orbital polarizabilities $\chi_b^{(n)}$ via an expansion of the bond-orbital electric dipole moment in the form

$$\langle b | e(x - x_0) | b \rangle = (e/2)(rd + q\Delta) = \sum_{n=0}^{\infty} \chi_b^{(n)} E_x^n, \quad (4.16)$$

it is now straightforward, using Eqs. (4.6) and (4.8)–(4.16), to calculate $\chi_b^{(n)}$ with $n = 1, 2, 3$ explicitly. For a discussion of linear response, as in this paper, we need only pursue $\chi_b^{(1)}$ via r_1 of Eq. (4.10) in the form

$$\chi_b^{(1)} = eAr_1\lambda/2E_x = e^2\alpha^3fA^2/4a^2V_2. \quad (4.17)$$

Using Eqs. (4.4) and (4.13) this expression takes on a final form

$$\chi_b^{(1)} = \frac{e^2\alpha^3f}{4(1 - S^2)V_2}(d + g\Delta)^2 \quad (4.18)$$

with

$$g = (S/\alpha)[(1 - \alpha^2)/(1 - S^2)]^{1/2}, \quad (4.19)$$

where “covalency” α is given, in terms of the original zero-field matrix elements V_2 and V_3 , by Eq. (2.16). Equations (4.11) and (4.12) are given here for future reference in a following paper.

Generally, for insulators (with high ionic coordination numbers) the primary bond orbitals are not independent and may not involve σ bonds. However, we show in the Appendix that, at least in the ionic limit $|b_0\rangle = |h_X\rangle$, each bond orbital does contribute independently to susceptibility. Moreover, in high-symmetry geometries, these contributions are equal and (see the Appendix) are proportional to the one-electron σ -bond susceptibility of Eq. (4.18) in such a way that the macroscopic electronic dielectric constant ϵ can be written as

$$\epsilon - 1 = (8\pi/3)zN_X\chi_b^{(1)}, \quad (4.20)$$

where there are z electrons per anion involved in the bonding ($z=6$ for the materials discussed in this paper) and N_X is the number of anions per unit volume. Although this independence of bond-orbital contribution to $\epsilon-1$ does not hold rigorously in high coordination if $|b_0\rangle \neq |h_X\rangle$, we shall assume Eq. (4.20) to be at least approximately valid for all the materials discussed in this paper.

For a compound of formula unit MX_n , and molar volume V_M , it follows that the final bond-orbital expression for ϵ can be cast as

$$\epsilon - 1 = 16\pi n(N_0/V_M)\chi_b^{(1)}, \quad (4.21)$$

where N_0 is Avogadro's number. Equivalently, using Eq. (4.18), this may be recast as

$$\epsilon - 1 = (Gn/V_M V_2)(d + g\Delta)^2, \quad (4.22)$$

where

$$G = 4\pi N_0 e^2 f \alpha^3 / (1 - S^2). \quad (4.23)$$

This result takes on a particularly simple form for the ionic limit $\alpha=S$ (which we shall assume to hold for all coordination halides), viz., $g=1$ and

$$\epsilon - 1 = (G'n/V_M V_2)(d + \Delta)^2, \quad \text{ionic} \quad (4.24)$$

with

$$G' = G_{\text{ionic}} = [4\pi N_0 e^2 f S^3 / (1 - S^2)] (6.24 \times 10^{-5}) \quad (4.25)$$

if, as from here and henceforth, d is expressed in Å, V_2 in eV, and V_M in cm^3 .

V. THE HALIDES

Our first test of the theory of linear electronic response given in the previous section will be carried out for the pretransition-metal halides. For these, the predominantly p -electron nature of the observed valence bands²⁵ points to a representation close to the ionic limit $\alpha=S$. Post-transition-metal halides are excluded at the present stage because the presence of d -electron contributions from relatively shallow d bands complicates the picture for this group of materials. Since frequency-dispersion effects have not been included in the formalism of Sec. IV, the experimental response ϵ relevant for comparison with the theoretical form Eq. (4.24) is that extracted from the electronic term of a single-oscillator Sellmeier dispersion relationship^{26,27} in the low-frequency limit. For wide-band-gap materials this will not differ greatly from from the square of the refractive index at visible frequencies, but for narrow-band-gap materials, it may be somewhat smaller.

In Table I we give values of ϵ for all the pretransition-metal halides (28 in all) for which we have located a Sellmeier analysis. Also shown in Table I are bond lengths d and molar volumes V_M (as calculated from their published crystal structures²⁸) and cationic radii.²⁹ We first consider Eq. (4.24) with Δ set equal to zero. This is the assumption that the mean position of cation-anion overlap x_0 along a bond is at the bond center $x_0 = d/2$

(Fig. 1). Plotting $\log(G'/V_2)$, as calculated from Eq. (4.24) with $\Delta=0$, against $\log(d)$ gives, for the alkali halides, the results shown in Fig. 2(a). The points for each separate cation lie on different straight lines of equal slope. This is essentially equivalent to a finding first established by Pantelides.⁷ However, we now note that the line positions are quite accurately dependent only on cation radius R_M . In particular, if in Eq. (4.24) we set

$$d + \Delta = d(d/2R_M)^{1/2}, \quad (5.1)$$

instead of $d + \Delta = d$, then the plot of $\log(G'/V_2)$ versus $\log(d)$ for all the 28 halides of Table I is quite accurately given [Fig. 2(b)] by a single linear relation [i.e., the separate straight lines of Fig. 2(a) fuse into a single resultant which also accommodates the other halides as well]. The condition Eq. (5.1), is just that of Eq. (3.7), which establishes how far from the bond center the location of x_0 is actually to be found. The electronic linear response for

TABLE I. The long-wavelength electronic dielectric constant ϵ (dimensionless), cation radius R_M (in Å), cation-anion bond length d (in Å), and molar volume V_M (in cm^3) for 28 pretransition-metal halides MX_n . (sc denotes simple cubic, rs denotes rocksalt.)

	Compound	Structure	ϵ	d	R_M	V_M
1	CsF	sc	2.15	3.00	1.69	25.13
2	CsCl	sc	2.63	3.57	1.69	42.21
3	CsCl	rs	2.30	3.57	1.69	54.83
4	CsBr	sc	2.79	3.71	1.69	47.42
5	CsBr	rs	2.43	3.71	1.69	61.60
6	CsI	sc	3.03	3.95	1.69	57.36
7	CsI	rs	2.63	3.95	1.69	74.51
8	RbF	rs	1.93	2.82	1.48	27.00
9	RbCl	rs	2.17	3.29	1.48	42.90
10	RbBr	rs	2.34	3.43	1.48	48.48
11	RbI	rs	2.59	3.67	1.48	59.59
12	KF	rs	1.84	2.67	1.33	23.02
13	KCl	rs	2.17	3.15	1.33	37.53
14	KBr	rs	2.35	3.30	1.33	43.29
15	KI	rs	2.63	3.53	1.33	53.11
16	NaF	rs	1.74	2.31	0.95	14.85
17	NaCl	rs	2.33	2.81	0.95	26.84
18	NaBr	rs	2.60	2.99	0.95	32.09
19	NaI	rs	2.98	3.24	0.95	40.83
20	LiF	rs	1.92	2.01	0.60	9.76
21	LiCl	rs	2.68	2.57	0.60	20.33
22	LiBr	rs	3.00	2.75	0.60	25.07
23	LiI	rs	3.4	3.00	0.60	32.45
24	MgF ₂	rutile	1.89	1.99	0.65	19.64
25	CaF ₂	fluorite	2.04	2.37	0.99	24.55
26	SrF ₂	fluorite	2.06	2.51	1.13	29.37
27	BaF ₂	fluorite	2.15	2.69	1.35	35.89
28	ZrF ₄	glass ^a	2.35	2.29	0.80	42.0

^aValues deduced from measurements on fluorozirconate glasses $(\text{ZrF}_4)_{1-x}(\text{BaF}_2)_x$.

these halides, therefore, from Eqs. (4.24) and (5.1), is given by

$$\epsilon - 1 = (G'/V_2)(nd^3/2V_M R_M), \quad (5.2)$$

where G'/V_2 satisfies the empiric power law [Fig. 2(b)]

$$G'/V_2 = d^{2.4}/4. \quad (5.3)$$

Combining Eqs. (5.2) and (5.3) now provides an extremely simple equation for the electronic dielectric constant of the pretransition-metal ionic halides MX_n , viz.,

$$\epsilon = 1 + (nd^{5.4}/8V_M R_M), \quad (5.4)$$

in which bond length d and cation radius R_M are in Å and the molar volume V_M is in cm^3 . The rms accuracy of this relationship over the 28 materials of Table I is 2.4% (or typically about 0.05 in ϵ) with a largest error of only 4.5%.

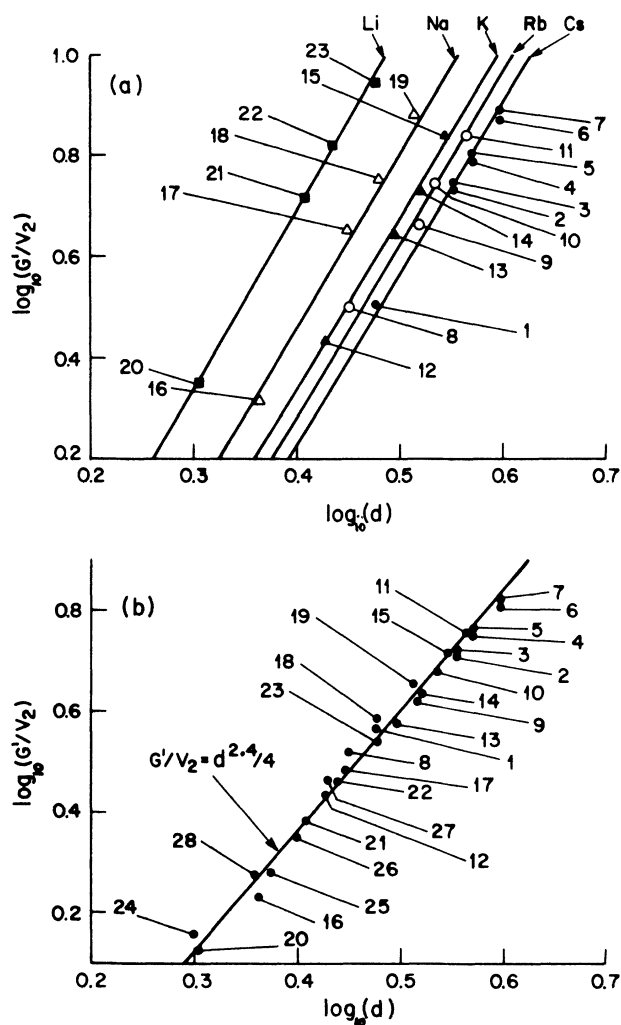


FIG. 2. (a) $\log(G'/V_2)$ vs $\log(d)$ as calculated from Eq. (4.24), for the alkali halides numbered in Table I, when parameter Δ is neglected (i.e., set equal to zero). (b) The same plot with Δ included and given by Eq. (5.1). In this plot we also include the additional non-alkali halides (Nos. 24–28) of Table I, and exhibit a fit to the analytic form $G'/V_2 = d^{2.4}/4$.

VI. CHALCOGENIDES

Having concluded that the pretransition-metal halides of Table I are all ionic, in the sense of having $\alpha \approx S$, we now turn to the pretransition-metal chalcogenides MX_n to see whether they also possess some common characteristic of an analogous kind. Writing $\alpha = \gamma S$, the Eq. (4.22) for ϵ can be re-expressed as

$$\epsilon - 1 = (G'\gamma^3 n/V_M V_2)(d + g\Delta)^2, \quad (6.1)$$

where G' is defined by Eq. (4.25), and

$$g^2 = (1 - \gamma^2 S^2)/[\gamma^2(1 - S^2)]. \quad (6.2)$$

Since we anticipate a larger degree of covalence for the anionically divalent ($Z_X = 2$) materials than for their halide ($Z_X = 1$) counterparts, we also anticipate for them deviations $\gamma > 1$ and $g < 1$ from the ionic limit $\gamma = g = 1$. Calculating Δ from Eq. (5.1), viz.,

$$\Delta = d[(d/2R_M)^{1/2} - 1], \quad (6.3)$$

we therefore also expect the $g\Delta$ term in Eq. (6.1) to have a less dramatic, though still significant, effect on the interpretation of their dielectric constant than it did for the halides.

In order to probe its significance, we once again first attempt a fit of experimental ϵ to Eq. (6.1) with Δ set equal to zero. We use experimental data (Table II) for all 16 relevant (i.e., high-coordination-number) chalcogenides for which the limiting long-wavelength electronic dielectric constant ϵ is known to us from the literature. The resulting plot of $\log(G'\gamma^3/V_2)$ versus $\log(d)$ is shown in Fig. 3(a) [and is to be compared with Fig. 2(a) for the halides]. Although the scatter is quite large, it is clear that a majority of points fall close to the line

TABLE II. As in Table I; for 16 high-coordination-number pretransition-metal chalcogenides.

	Compound	Structure	ϵ	d	R_M	V_M
1	BaO	rs	3.68	2.76	1.35	25.4
2	BaS	rs	4.26	3.19	1.35	39.1
3	BaSe	rs	4.48	3.30	1.35	43.3
4	BaTe	rs	4.71	3.49	1.35	51.3
5	SrO	rs	3.35	2.58	1.13	20.7
6	SrS	rs	4.09	3.01	1.13	32.9
7	SrSe	rs	4.33	3.12	1.13	36.6
8	SrTe	rs	4.91	3.24	1.13	40.8
9	CaO	rs	3.27	2.41	0.99	16.8
10	CaS	rs	4.24	2.85	0.99	27.7
11	CaSe	rs	4.58	2.96	0.99	31.1
12	MgO	rs	2.95	2.10	0.65	11.2
13	MgS	rs	4.84	2.60	0.65	21.2
14	MgSe	rs	5.28	2.73	0.65	24.4
15	AlO _{1.5}	corundum	3.07	1.92	0.50	12.8
16	LiO _{0.5}	antifluorite	2.65	2.00	0.60	7.4

$$G'\gamma^3/V_2 = 0.8d^{2.4} \quad (6.4)$$

[see Fig. 3(a)] which, on comparison with Eq. (5.3) extracted for the halides, points to a value of $\gamma^2 \approx 2$ as relevant for the chalcogenides of Table II. We also note that the four compounds (viz., MgS, MgSe, $\text{AlO}_{1.5}$, and Li_2O) which deviate most markedly from Eq. (6.4) are just those for which the ratio d/R_M is largest and for which, therefore, the heretofore neglected $g\Delta$ contribution to Eq. (6.1) will be most significant.

With γ^2 of order 2, we see from Eq. (6.2) that the parameter g is not overly sensitive to S for physically realistic values of overlap ($S^2 \ll 1$) taking on a value a little less than $1/\sqrt{2}$. Although its precise value is not critical, since $g\Delta/d \ll 1$ throughout, we can in fact look ahead to the self-consistently determined overlap values of the following section (Table IV) to estimate the narrow range $g = 0.65 \pm 0.02$. With this value ($g = 0.65$), and Δ as calculated from Eq. (6.3), we now replot $\log(G'\gamma^3/V_2)$ versus $\log(d)$ using the full formalism of Eq. (6.1) and the

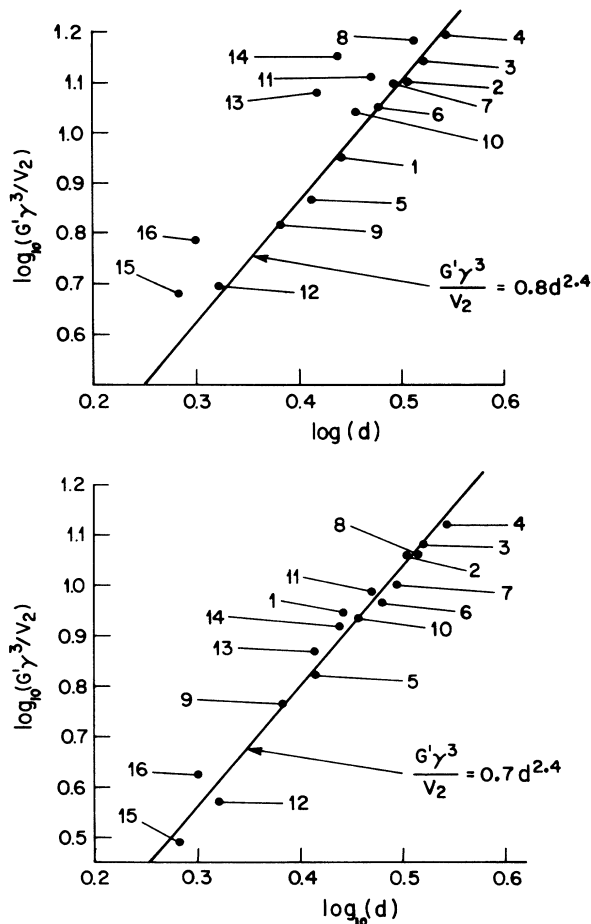


FIG. 3. (a) $\log(G'\gamma^3/V_2)$ vs $\log(d)$ as calculated from Eq. (6.1), for the chalcogenides numbered in Table II, when parameter Δ is neglected (i.e., set equal to zero). (b) The same plot with Δ included, and given by Eq. (5.1), or equivalently Eq. (6.3), and $g = 0.65$. Also shown (solid line) is the fit to the analytic form $G'\gamma^3/V_2 = 0.70d^{2.4}$.

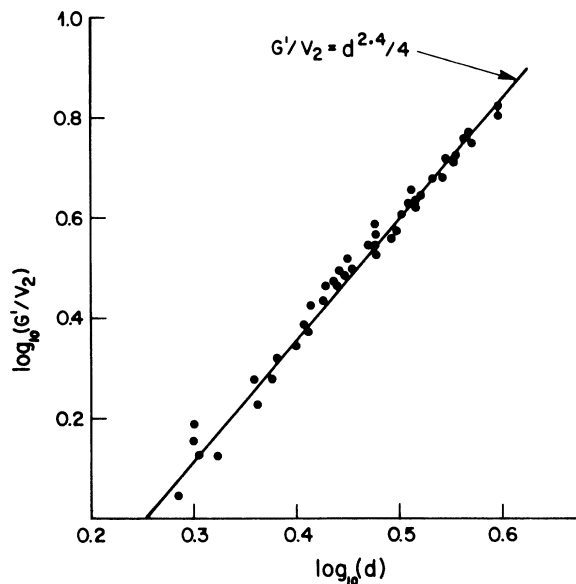


FIG. 4. A plot of $\log(G'/V_2)$ vs $\log(d)$ as calculated (see text) from Eq. (6.1) for all 44 material listed in Tables I and II, exhibiting the universal fit to the relationship $G'/V_2 = d^{2.4}/4$.

data of Table II. The result is shown in Fig. 3(b) [compare Fig. 2(b) for the halides]. The linearity of the logarithmic plot, establishing the quantitative form

$$G'\gamma^3/V_2 = 0.70d^{2.4}, \quad (6.5)$$

is now striking. The rms accuracy of the implied relationship

$$\epsilon = 1 + (0.70nd^{2.4}/V_M)(d + 0.65\Delta)^2, \quad (6.6)$$

over 16 materials in Table II is 5.0%.

Comparing Eqs. (5.3) and (6.5), we conclude that $\gamma^2 = 1.99$. We may therefore say, with considerable precision, that the chalcogenides of Table II all possess a "covalency measure" $\alpha = \sqrt{2}S$, which is to be compared with the ionic limit $\alpha = S$ valid for the pre-transition-metal halides (and a fully covalent limit $\alpha = 1$ determined by definition). It follows that we can cover all the crystals in Tables I and II with the common covalency criterion

$$\alpha = (Z_X)^{1/2}S, \quad (6.7)$$

in which Z_X is the magnitude of the formal anion valence. Finally, combining the halide and chalcogenide results by use of Eq. (6.1) with $\gamma^2 = 1, 2$ and $g = 1, 0.65$ for $Z_X = 1, 2$, respectively, now enables us to plot $\log(G'/V_2)$ versus $\log(d)$ for all 44 compounds of Tables I and II together. The result, shown on Fig. 4 reveals an impressive fit to $G'/V_2 = d^{2.4}/4$ of Eq. (5.3) throughout.

VII. THE COMPLETE PARAMETRIZATION

In spite of the success of the bond-orbital method to this point, we have not yet determined the complete set of defining parameters (f , S , V_2 , V_3 , M , E_0 , etc.) intro-

duced in Sec. II for any crystal. Indeed, such a complete parametrization cannot be carried out with full self-consistency at the linear-response level alone. However, the task can be completed by pursuing the nonlinear response as set out in our following paper, and the essential finding is a very simple one which can easily be included at this juncture. It is that the local-field parameter f in the context of bond orbitals is essentially equal to unity for the halides and is (at least) quite close to unity even for the more polarizable chalcogenides. Physically, this lack of local-field enhancement is presumably due to the extended nature of the electronic orbitals involved in the theory—the commonly used Lorentz condition $f = f_L = (\epsilon + 2)/3$ for cubic materials being rigorously valid only in the unphysical limit of point dipoles.

Setting $f = 1$ we now have only two independent quantities left to be determined. If we choose them to be V_2 and S , then all the other bond-orbital parameters of Sec. II follow from them immediately in the fashion

$$M = V_2(1 - S^2), \quad (7.1)$$

$$\alpha = (Z_X)^{1/2} S, \quad (7.2)$$

$$V_3 = V_2(1 - \alpha^2)^{1/2} / \alpha, \quad (7.3)$$

$$E_0 = V_2[(1 - \alpha^2)(1 - S^2)]^{1/2} / \alpha. \quad (7.4)$$

To determine V_2 and S we require two independent relations involving only V_2 and S and known or measurable quantities. One has already been written in the form $G'/V_2 = d^{2.4}/4$ which, making use of the definition of G' as given in Eq. (4.25), acquires the explicit form

$$\frac{436fS^3}{V_2(1 - S^2)} = d^{2.4}, \quad (7.5)$$

in which we have used the values $e = 4.8 \times 10^{-10}$ esu and $N_0 = 6.023 \times 10^{23}$, and where V_2 is in eV and d in Å. The second comes from the bonding-antibonding energy gap E_s , calculated by subtracting the two solutions

$$E = SV_2 \pm (V_2^2 + V_3^2)^{1/2} \quad (7.6)$$

of Eq. (2.8). Using the definition of Eq. (2.16) for covalency α , it may be expressed in the extremely simple form

$$E_s = 2V_2 / \alpha, \quad (7.7)$$

which, when combined with Eq. (7.5), provides the relationship

$$\frac{872fS^3}{(1 - S^2)\alpha E_s} = d^{2.4}. \quad (7.8)$$

With $f = 1$ and $\alpha = (Z_X)^{1/2} S$ this can be recast as

$$E_s = \frac{872S^2}{(1 - S^2)(Z_X)^{1/2} d^{2.4}} \quad (7.9)$$

with E_s in eV and d in Å.

The importance of this equation is that E_s is actually an observable and appears in the *frequency-dependent* linear response $\epsilon(\omega)$. If the applied field E_x in Sec. IV is

assumed to be time dependent in the fashion $E_x \sim \exp(i\omega t)$, then the lowest-order frequency response for such a two-level system with an unperturbed energy splitting E_s is well known (from time-dependent perturbation theory³⁰) to depend on frequency via the factor $(E_s^2 - \hbar^2\omega^2)^{-1}$. The static response of Eq. (4.22) is therefore readily adapted for frequency dependence in the fashion

$$\epsilon(\omega) - 1 = \frac{GnE_s^2(d + g\Delta)^2}{V_M V_2(E_s^2 - \hbar^2\omega^2)} \quad (7.10)$$

which, of course, reduces to Eq. (4.22) as $\omega \rightarrow 0$.

A single frequency dispersion form of this kind (with a frequency-independent energy gap E_s) is, in optical literature, referred to as a Sellmeier dispersion with E_s being the electronic "Sellmeier energy." It accurately describes actual linear response dispersion if $\hbar\omega \ll E_s$, provided that ω is well above the highest phonon frequencies. It follows that E_s can be directly determined from experiment^{26,27,31} Insertion into Eq. (7.9) now directly determines the overlap integral S , and the rest of the bond orbital parameters follow immediately via Eqs. (7.1) to (7.4)

TABLE III. The measured Sellmeier energy gap E_s and the bond-orbital parameters derived from it via Eqs. (7.1)–(7.4), (7.7), and (7.9) for the crystalline pretransition-metal halides of Table I.

Crystal (Units)	E_s (eV)	$\alpha = S$	V_2 (eV)	V_3 (eV)	M (eV)	$2E_0$ (eV)
CsF (sc)	14.3	0.43	3.1	6.5	2.5	11.6
CsCl (rs&sc)	10.5	0.45	2.4	4.7	1.9	8.4
CsBr (rs&sc)	9.4	0.45	2.1	4.2	1.7	7.5
CsI (rs&sc)	7.7	0.44	1.7	3.5	1.4	6.2
RbF (rs)	14.5	0.41	3.0	6.6	2.5	12.1
RbCl (rs)	10.4	0.41	2.2	4.7	1.8	8.6
RbBr (rs)	9.3	0.41	1.9	4.2	1.6	7.7
RbI (rs)	7.8	0.41	1.6	3.6	1.3	6.5
KF (rs)	14.7	0.39	2.9	6.8	2.4	12.5
KCl (rs)	10.5	0.40	2.1	4.8	1.8	8.8
KBr (rs)	9.2	0.39	1.8	4.2	1.5	7.8
KI (rs)	7.6	0.39	1.5	3.5	1.3	6.4
NaF (rs)	15.1	0.34	2.6	7.1	2.3	13.4
NaCl (rs)	10.5	0.35	1.9	4.9	1.6	9.2
NaBr (rs)	9.1	0.35	1.6	4.3	1.4	8.0
NaI (rs)	7.4	0.35	1.3	3.5	1.1	6.5
LiF (rs)	16.5	0.30	2.5	7.9	2.3	15.0
LiCl (rs)	11.0	0.33	1.8	5.2	1.6	9.8
LiBr (rs)	9.5	0.33	1.6	4.5	1.4	8.5
LiI (rs)	8.0	0.34	1.4	3.8	1.2	7.1
MgF ₂ (rutile)	16.8	0.30	2.5	8.0	2.3	15.3
CaF ₂ (fluorite)	15.7	0.35	2.8	7.3	2.4	13.7
SrF ₂ (fluorite)	14.7	0.36	2.7	6.8	2.3	12.7
BaF ₂ (fluorite)	13.8	0.38	2.6	6.4	2.3	11.8

TABLE IV. As in Table III but for high-coordination-number pretransition-metal chalcogenides. All have rocksalt structure except for Al_2O_3 (corundum).

Crystal (units)	E_s (eV)	S	α	V_2 (eV)	V_3 (eV)	M (eV)	$2E_0$ (eV)
BaO	7.1	0.34	0.48	1.7	3.1	1.5	5.9
BaS	6.3	0.38	0.53	1.7	2.7	1.4	4.9
BaSe	5.3	0.36	0.51	1.4	2.3	1.2	4.2
BaTe	4.2	0.35	0.49	1.0	1.8	0.9	3.4
SrO	8.3	0.34	0.48	2.0	3.6	1.8	6.8
SrS	6.6	0.36	0.51	1.7	2.8	1.5	5.3
SrSe	5.4	0.34	0.49	1.3	2.4	1.2	4.4
SrTe	4.9	0.34	0.49	1.2	2.1	1.1	4.0
CaO	9.9	0.34	0.48	2.4	4.3	2.1	8.1
CaS	6.9	0.35	0.49	1.7	3.0	1.5	5.6
CaSe	5.6	0.33	0.47	1.3	2.5	1.2	4.7
MgO	11.4	0.31	0.44	2.5	5.1	2.3	9.7
MgS	7.6	0.33	0.47	1.8	3.4	1.6	6.4
MgSe	7.0	0.34	0.47	1.7	3.1	1.5	5.8
Al_2O_3	13.4	0.31	0.43	2.9	6.0	2.6	11.5

and (7.7). Taking E_s values from Wemple,³¹ we calculate all these bond-orbital parameters both for the halides and chalcogenides of relevance to this paper; the detailed results are given in Table III and IV. Our only comment on the values is that the suggestion by Harrison^{9,32} that the intraband matrix elements (M) and "band gap" $2E_0$ (or E_s) should scale absolutely as $1/d^2$ for s - p bonding, though at least approximately valid for the chalcogenide series, is not confirmed for the halides. For the latter an approximate d^{-2} dependence is observed separately for each cation, but the amplitude is grossly cation dependent. Note also (Table III) that overlap is largely determined by cation type alone for the alkali halides.

VIII. CONCLUSIONS

Our most important conclusion is that all the bond-orbital findings for linear response can be combined into a single formula as follows: the limiting long-wavelength electronic dielectric constant ϵ for all binary pretransition-metal halides and chalcogenides MX_n (excepting only those, like BeF_2 , which contain hybridized orbitals leading to low coordination numbers and directed valence) can be expressed as

$$\epsilon = 1 + (Z_X^{1.5} n d^{2.4} / 4V_M) (d + g\Delta)^2 \quad (8.1)$$

in which

$$\Delta = d [(d/2R_M)^{1/2} - 1], \quad (8.2)$$

and $g=1$ for halides and $g=0.65$ for chalcogenides. In these equations, d is the bond length (in \AA), V_M is the molar volume (in cm^3), R_M is cation radius (in \AA), and Z_X is the formal anion valence magnitude (i.e., one for halides, two for chalcogenides).

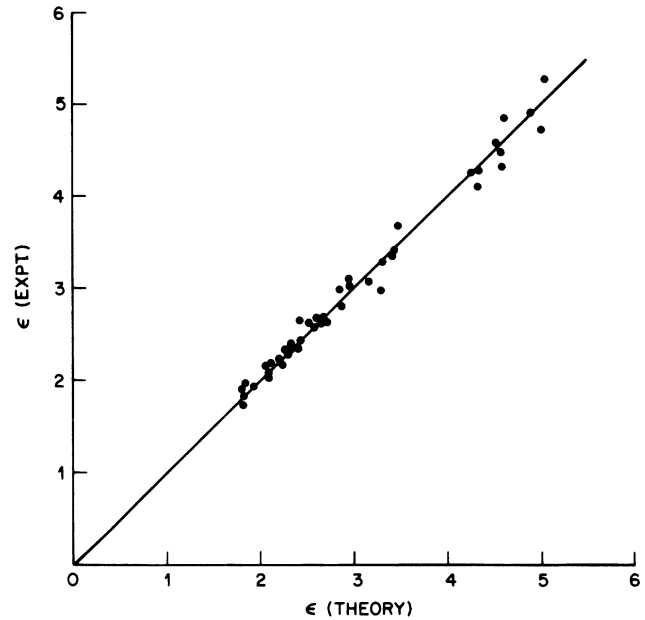


FIG. 5. A direct comparison of theory [Eq. (8.1)] and experiment for the electronic dielectric constant ϵ of the 44 halides and chalcogenides of Tables I and II.

The accuracy of Eq. (8.1) over the 44 relevant compounds for which ϵ is presently known to us (see Tables I and II) is indicated in Fig. 5 where we directly plot the experimental values against the theoretical predictions following from Eq. (8.1). The overall accuracy is close to a rms value of 3.4%. For the halides alone (i.e., $Z_X=1$, $g=1$) the Eq. (8.1) reduces to the even simpler form

$$\epsilon = 1 + (nd^{5.4} / 8V_M R_M), \quad \text{halides} \quad (8.3)$$

which is (rms) accurate to about 2.4% over the 28 halides of Table I.

The other parameters which define the bond-orbital model, but which do not appear explicitly in the final expression for linear response, have all been numerically determined for each halide and chalcogenide. They include interionic and intraionic one-electron matrix elements (V_2 , M , V_3 , and E_0 as defined in Sec. II) and also the overlap integral S between valence- and conduction-electron orbitals on neighbor sites. Detailed numerical values are given in Tables III and IV. Incorporated into these calculations is the finding of our following paper on nonlinear response (II) that local-field effects in the context of bond-orbital theory are essentially absent throughout; or $f=1$ in the nomenclature of Sec. IV.

APPENDIX

Consider an anionic p_x orbital $|p_x\rangle$ overlapping m equivalent cationic (nearest neighbor) s orbitals $|s_i\rangle$, $i=1,2,\dots,m$ as shown in Fig. 6. The s orbitals are equivalent as regards their intraorbital matrix elements, but, at this junction, no geometric restrictions are assumed concerning their relative orientational locations

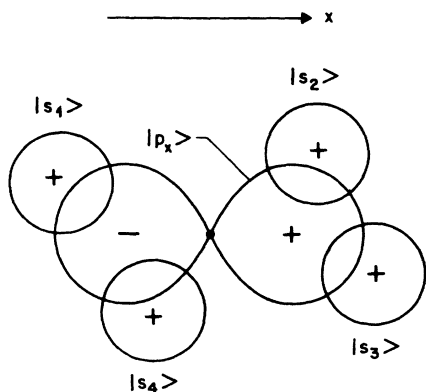


FIG. 6. Schematic of an anion p_x orbital $|p_x\rangle$ overlapping four equivalent cation s orbitals $|s_i\rangle$, $i=1-4$.

with respect to the x axis of the p_x orbital. Choosing the zero of energy such that

$$\begin{aligned} \langle p_x | \mathcal{H}_0 | p_x \rangle &= -E_0, \\ \langle s_i | \mathcal{H}_0 | s_j \rangle &= +E_0 \delta_{ij}, \end{aligned} \quad (\text{A1})$$

where \mathcal{H}_0 is a one-electron Hamiltonian, we ignore all interactions between different cations. The sole remaining interactions, between the p_x orbital and the cations, are then included by defining the relevant one-electron matrix elements

$$\langle p_x | \mathcal{H}_0 | s_i \rangle = -M_i. \quad (\text{A2})$$

These equations, for $i=1,2,\dots,m$, together with the following orbital overlap relationships:

$$\begin{aligned} \langle p_x | s_i \rangle &= S_i, \\ \langle s_i | s_j \rangle &= \delta_{ij}, \\ \langle p_x | p_x \rangle &= 1, \end{aligned} \quad (\text{A3})$$

define a bond-orbital system for which the ground state can be expressed most generally in the form

$$b = c|p_x\rangle + \sum_i a_i |s_i\rangle. \quad (\text{A4})$$

The coefficients c and a_i can be obtained variationally by minimizing the one-electron energy $\langle b | \mathcal{H}_0 | b \rangle / \langle b | b \rangle$ with respect to them. In order to investigate the response of such a system to an applied field E_x in the x direction we include a field-energy term viz., $\mathcal{H} = \mathcal{H}_0 - \lambda x$, where

$$\lambda = efE_x \quad (\text{A5})$$

in which e is electronic charge, and f incorporates any local-field enhancement or shielding effects. Minimizing the energy

$$E = \frac{\langle b | (\mathcal{H}_0 - \lambda x) | b \rangle}{\langle b | b \rangle} \quad (\text{A6})$$

with respect to the coefficients c and a_i of Eq. (A4) provides the matrix relationship

$$\begin{pmatrix} A_0 & A_1 & A_2 & A_3 & \cdots & A_m \\ A_1 & B_1 & 0 & 0 & \cdots & 0 \\ A_2 & 0 & B_2 & 0 & \cdots & 0 \\ A_3 & 0 & 0 & B_3 & \cdots & 0 \\ \vdots & \vdots & \vdots & \vdots & \cdots & \vdots \\ A_m & 0 & 0 & 0 & \cdots & B_m \end{pmatrix} \begin{pmatrix} c \\ a_1 \\ a_2 \\ a_3 \\ \vdots \\ a_m \end{pmatrix} = \begin{pmatrix} 0 \\ 0 \\ 0 \\ 0 \\ \vdots \\ 0 \end{pmatrix}, \quad (\text{A7})$$

in which

$$\begin{aligned} A_0 &= E + E_0 \\ A_i &= M_i + ES_i + \lambda \langle p_x | x | s_i \rangle, \quad i=1,2,\dots,m, \\ B_i &= E - E_0 + \lambda \langle s_i | x | s_i \rangle, \quad i=1,2,\dots,m. \end{aligned} \quad (\text{A8})$$

The simplest solutions for c and a_i from Eq. (A7) arise for the case of fully ionic systems, defined in terms of a fully occupied p_x orbital and empty s_i orbitals in the absence of the field. For this case, we can write

$$M_i - E_0 S_i = 0, \quad i=1,2,\dots,m \quad (\text{A9})$$

corresponding to the zero-field condition $c=1$, $a_i=0$, $E=-E_0$, and $|b\rangle=|p_x\rangle$. For this ionic limit we can expand E and a_i , in the presence of a field, as power series in λ . Including, for our present purposes, only terms up to first order, we write

$$\begin{aligned} E &= -E_0 + \lambda E', \\ a_i &= \lambda a'_i, \quad i=1,2,\dots,m \end{aligned} \quad (\text{A10})$$

in terms of which the matrix elements of Eqs. (A8) reduce to

$$\begin{aligned} A_0 &= \lambda E', \\ A_i &= \lambda [E' S_i + \langle p_x | x | s_i \rangle], \quad i=1,2,\dots,m, \\ B_i &= -2E_0 + \lambda [E' + \langle s_i | x | s_i \rangle], \quad i=1,2,\dots,m. \end{aligned} \quad (\text{A11})$$

With these values Eq. (A7) is readily solved to first order in λ to give $E'=0$, $c=1$ (for a normalized wave function), and

$$a'_i = \langle p_x | x | s_i \rangle / 2E_0, \quad i=1,2,\dots,m. \quad (\text{A12})$$

The resulting field-dependent bonding orbital, therefore, takes the form

$$|b'\rangle = |p_x\rangle + \sum_i \lambda [\langle p_x | x | s_i \rangle / 2E_0] |s_i\rangle \quad (\text{A13})$$

while the corresponding field-induced dipole moment follows as

$$\mu_x(p_x) = \langle b' | ex | b' \rangle / \langle b' | b' \rangle = e^2 f E_x \sum_i \langle p_x | x | s_i \rangle^2 / E_0. \quad (\text{A14})$$

The important feature is that $\mu_x(p_x)$ is the sum of *independent* contributions from each of the surrounding cations. Although, in general, there will also be contributions to field-induced dipole moment μ_x from the other p orbitals as follows:

$$\begin{aligned}\mu_x(p_y) &= e^2 f E_x \sum_i \langle p_y | x | s_i \rangle^2 / E_0, \\ \mu_x(p_z) &= e^2 f E_x \sum_i \langle p_z | x | s_i \rangle^2 / E_0,\end{aligned}\quad (\text{A15})$$

the independence of the separate cationic contributions remains.

In a highly symmetric environment which is unable to lift the p -orbital degeneracy we are free to choose the absolute orientational configuration of the orbital triplet $|p_x\rangle, |p_y\rangle, |p_z\rangle$ at will. Let us choose them, for an arbitrarily chosen cation i , in a manner which places the x axis along the vector connecting the anion nucleus to the nucleus of this cation. In this case, we have $\langle p_y | x | s_i \rangle = \langle p_z | x | s_i \rangle = 0$, so that the total contribution of $|s_i\rangle$ to induced dipole moment μ_x takes the particularly simple form

$$(\mu_x)_i = e^2 f E_x \langle p_x | x | s_i \rangle^2 / E_0. \quad (\text{A16})$$

It follows that we can define a unique linear polarizability $\chi_b^{(1)} = (\mu_x)_i / E_x$ per bonding-orbital electron parallel to each bond i .

The weight to be associated with each bond must be proportional to z/m which, when summed over the num-

ber of bonds m per anion, gives the number z of electrons available for bonding per anion. The bulk optical frequency dielectric constant then follows as

$$\epsilon = 1 + 4\pi \frac{1}{3} p z N_A \chi_b^{(1)} \quad (\text{A17})$$

where there are N_A anions per unit volume, p is the proportionality factor, and the $\frac{1}{3}$ arises from an angular average over bond directions assuming a high-symmetry anionic environment. The factor p is readily determined to have the value two by analyzing the simplest case of an octahedral coordination (e.g., rocksalt) and field applied along a bond axis, viz.,

$$\epsilon = 1 + 4\pi N_A (4\chi_b^{(1)}) \quad (\text{A18})$$

since $z=6$ for p orbitals. Assuming the value $z=6$ to be appropriate for all the insulators discussed in this paper, the equation (A17) for a compound of formula unit MX_n (M =cation, X =anion) can now be more conveniently expressed in the form

$$\epsilon = 1 + 16\pi n (N_0 / V_M) \chi_b^{(1)} \quad (\text{A19})$$

in which N_0 is Avogadro's number, and V_M is the molar volume. This is the Eq. (4.21) of the text.

¹See, for example, C. Kittel, *Introduction to Solid State Physics*, 6th ed. (Wiley, New York, 1986), p. 368ff.

²J. C. Sharma and J. Shanker, *Phys. Rev. B* **19**, 6604 (1979).

³N. Dutt and G. G. Agrawal, *Solid State Commun.* **55**, 993 (1985).

⁴G. D. Mahan, *Phys. Rev. B* **34**, 4235 (1986).

⁵R. Adair, L. L. Chase, and S. A. Payne, *Phys. Rev. B* **39**, 3337 (1989).

⁶M. D. Johnson, K. B. Subbaswamy, and G. Senatore, *Phys. Rev. B* **36**, 9202 (1987).

⁷S. T. Pantelides, *Phys. Rev. Lett.* **35**, 250 (1975).

⁸J. C. Slater, *The Self-Consistent Field for Molecules and Solids* (McGraw-Hill, New York, 1974), Vol. 4.

⁹W. A. Harrison, *Electronic Structure and the Properties of Solids* (Freeman, San Francisco, 1980).

¹⁰K. H. Johnson, J. G. Norman, Jr., and J. W. D. Connolly, in *Computational Methods for Large Molecules and Localized States in Solids*, edited by F. A. Herman (Plenum, New York, 1973).

¹¹V. L. Moruzzi, J. F. Janak, and A. R. Williams, *Calculated Electronic Properties of Metals* (Pergamon, New York, 1978).

¹²J. R. Chelikowski and M. L. Cohen, *Phys. Rev. B* **14**, 556 (1976).

¹³C. S. Wang and B. M. Klein, *Phys. Rev. B* **24**, 3393 (1981).

¹⁴N. E. Christensen, S. Satpathy, and Z. Pawlowska, *Phys. Rev. B* **36**, 1032 (1987).

¹⁵C. A. Coulson, L. R. Redei, and D. Stocker, *Proc. R. Soc. London, Ser. A* **270**, 357 (1962).

¹⁶R. Hoffmann, *J. Chem. Phys.* **39**, 1397 (1963).

¹⁷J. C. Phillips, *Rev. Mod. Phys.* **42**, 317 (1970).

¹⁸J. C. Phillips, *Bonds and Bands in Semiconductors* (Academic,

New York, 1973).

¹⁹J. A. Van Vechten, *Phys. Rev.* **182**, 891 (1969); **187**, 1007 (1969).

²⁰W. A. Harrison, *Phys. Rev. B* **8**, 4487 (1973).

²¹W. A. Harrison and S. Ciraci, *Phys. Rev. B* **10**, 1516 (1974).

²²W. A. Harrison, *Phys. Rev. B* **14**, 702 (1976).

²³M. E. Lines and J. V. Waszczak, *J. Appl. Phys.* **48**, 1395 (1977).

²⁴S. T. Pantelides and W. A. Harrison, *Phys. Rev. B* **13**, 2667 (1976).

²⁵S. T. Pantelides, *Phys. Rev. B* **11**, 5082 (1975).

²⁶S. H. Wemple and M. DiDomenico, Jr., *Phys. Rev. B* **3**, 1338 (1971).

²⁷S. H. Wemple, *Phys. Rev. B* **7**, 3767 (1973).

²⁸R. W. G. Wyckoff, *Crystal Structures* (Krieger, Malabar, Florida, 1982), Vol. 1.

²⁹Commonly tabulated ionic-radius values (such as given, for example, in the *Table of Periodic Properties of the Elements* (Sargent-Welch, Chicago, 1962) suffice. Coordination-correlated values [see, for example, R. D. Shannon, *Acta Cryst. A* **32**, 751 (1976)] seem to have no greater success in matching the required $R_M + R_X = d$ for the materials of Tables I and II and, in any event, provide "corrections" which are small to the point of irrelevance in the present context.

³⁰A. Davydov, *Quantum Mechanics* (Pergamon, Oxford, 1965), p. 316ff.

³¹S. H. Wemple, *J. Chem. Phys.* **67**, 2151 (1977). Note that Wemple's E_0 is equivalent to our E_s .

³²W. A. Harrison, *Comments Condensed Matter Phys.* **13**, 177 (1987).